Supplementary document

Embedded carbon dots mediator in Ce-MoO_{3-x} heterojunction for improved visible-light driven N_2 fixation: Performances and interfacial activation mechanism

Huaiwei Zhang[a]*, Liang Bao[a], Ying Pan[a], Lulu Xu[b]*, Wei Wang[c]

[a] College of Materials and Environmental Engineering, Hangzhou Dianzi University, Hangzhou 310018, PR China

[b] School of Chemical Engineering, University of New South Wales, Sydney, NSW 2052, Australia

[c] School of Engineering, RMIT University, Melbourne, VC 3001, Australia

*Corresponding authors. E-mail: zhw5984@hdu.edu.cn (H.Zhang), lulu.xu1@unsw.edu.au (L.Xu)

Chemicals:

Mo powder (80 nm, > 99.9%) and H_2O_2 solution (3 wt. % in pure H_2O) were obtained from Macklin Ltd. (Shanghai, China). Cerium chloride hexahydrate ($CeCl_3 \cdot 6H_2O$, > 99.9 %), glucose ($C_6H_{12}O_6$, > 98%), Ethylene glycol ($C_2H_6O_2$, > 99.8%), potassium sodium tartrate tetrahydrate ($KNaC_4H_{12}O_{10} \cdot 4H_2O$) and Nessler's reagent (K_2HgI_4) were purchased from Aladdin Ltd. (Shanghai, China). The purity Argon (Ar) and purity nitrogen (N_2) were obtained from Minxing Huagong Technology Co., Ltd. (Hangzhou, China). All chemicals were of analytical grade and used without further purification.

Characterization

Phase and crystal structures of the photo-catalysts are measured via XRD method (X-ray diffractometer, MinFlex600, Rigaku, Japan). Surface and interface electronic states are detected through XPS measurement. (Thermo Scientific K-Alpha, Thermo Scientific Ltd, USA). The accurate element contents are determined by inductively coupled plasma-atomic emission spectrometry method (ICP-AES, PerkinElmer). The crabon and nitrogen contents in the catalysts are detected by elements analyzer (Multi EA S 5000, Analytik Jena AG, Germany). The microstructures are observed via the TEM analyses (JEOL JEM-2100F, Japan). DRS curves are detected by the UV-vis

diffuse reflectance spectra (UV-3600 UV-vis spectrometer, Shimadzu, Japan). Raman spectra are obtained on a spectrometer (inVia Qontor, Renishaw, UK) with 532 nm laser excitation at room temperature. EPR signal curves are observed on an EPR detector (A300-10/12, Bruker, Germany). Photoluminescence spectra (PL) are detected through a fluorescent spectrometer (FLs1000/FS5, Edinburgh Instruments Ltd., UK) at excitation wavelength of 325nm. N_2-TPD (Nitrogen temperature programmed desorption) curves are measured on an automatic chemisorption instrument (AutoChem II 2920, Micromeritics, USA), and the signal is captured via the thermal conductivity detector (TCD). Photocurrent (I-t) and Mott-Schottky (M-S) curves are received from an electrochemical station (CHI 760E, Shanghai Chenhua, China) in the electrolyte of 0.5M Na_2SO_4 aqueous. ITO electrodes covered with the photocatalysts are applied as the working electrodes, the Ag/AgCl electrode is used as the reference, and the Pt electrode is as the counter. The light source is from a 300 W Xe lamp. The specific details are shown in the supported documents.

Ammonia detection process

In order to establish the absorbance-concentration standard curve, 20 mL standard NH_4Cl solution with the concentrations of 0, 5, 10, 20, 50 and 100 $\mu mol \cdot L^{-1}$ were mixed with 1 mL potassium sodium tartrate solution (500 $g \cdot L^{-1}$) and 1.5 mL Nessler's reagent, respectively. After standing 10 min, 5 mL of the above solution was used for a UV-vis absorbance measurement at 420 nm. The standard curve between the concentrations and the absorbance value was fitted, and the ammonia concentrations during the N_2 photo-fixation process were obtained according to the standard curve.

Nitrogen isotopic labeling experiments

^{15}N isotopic labeling experiments were performed in a closed quartz reaction reactor (30 ml). 20 mL of deionized water with 10 mg of photocatalysts (CCM) are concentrated into the reactor. Before the light irradiation, high-purity Ar is firstly bubbled in the reaction solution for 30 min at a speed of 100ml/min. Then 10 ml of high-purity $^{15}N_2$ gas is injected into the solution every 0.5 h under lighting. After 5-h illumination, the reaction solution is centrifuged to remove the solids. The PH of

supernatant is adjusted to 2 with HCl, followed by the addition of DMSO-d6. The obtained $^{15}NH_4^+$ is quantitatively confirmed with a Bruker Avance NEO 600 NMR spectrometer.

Determination of hydrazine:

The by-product of hydrazine during N_2 fixation process is detected by Watt-Chrisp method [1, 2]. A mixture of 6g para-(dimethylamino) benzaldehyde, 30 mL HCl (concentrated), and 300 mL ethanol solutions are applied to the color reagent. And then 2 mL standard hydrazine solution was transferred into the colorimetric tube, followed by adding 2 mL color reagent. After standing 30 min, the concentration of N_2H_4 was determined according to the absorbance at 455 nm on a UV-vis absorbance measurement. The standard curve can be obtained by linear regression of the concentrations and the absorbance value, and the hydrazine yields were estimated from a standard curve using 2 mL of clear reaction solution and 2 mL of color reagent.

Nitrogen temperature programmed desorption test

Nitrogen temperature programmed desorption (N_2-TPD) curves are measured on the Micromeritics AutoChem II 2920 apparatus. The catalysts are heat-treated under the flowing He gas at 200^{o}C for 1h firstly, and cool down to 50 ^{o}C. The N_2 absorption is operated in pure N_2 with a flowing rate of 50 ml·min^{-1} for 1 h. Then, the residual N_2 is removed through purging with He gas for another 1h. The N_2 desorption is processed by heating the sample from 50 to 800°C with the rate of 10 °C·min^{-1}. The signal is captured via the thermal conductivity detector (TCD).

FTIR tests

The FTIR spectra during the photocatalytic N_2 fixation process are obtained in laboratory at regular intervals. In brief, 100mg as-prepared CCM catalyst and 250 ml ultra-pure water are added into in a quartz reactor, and dispersed with ultrasonic for 1h in dark. The catalyst suspension is stirred using high pure N_2 at a flow rate of 20mL·min^{-1} for 15 min, and then irradiated under full spectrum irradiation with continued N_2 bubbling for 1h. During the reaction process, 50ml solution is extracted from the reactor at 0 min, 2 min, 5 min, 10 min 15 min and 60min, and the catalysts are separated from the sampled solutions. Finally, the precipitates are dried at 313K

overnight under N_2 atmosphere. The obtained samples are analyzed through a Nicolet iS10 FTIR spectrometer, respectively.

Electrochemical measurement

The M-S and I-t curves are obtained on an electrochemical station (CHI 760E Shanghai Chenhua, China) using as-prepared working electrodes. The Mott-Schottky (M-S) curves are measured from -1.0~0.2 V vs.Ag/AgCl reference electrode at the frequency of 1000Hz on the electrochemical station (CHI 760E Shanghai Chenhua, China) in the electrolyte of 0.5M Na_2SO_4 aqueous. The electrolyte is bubbled with nitrogen for 20 min before the measurements. I-t curves are measured at the initial potential of 0.5 V with the interval of 0.1 s in Ar or N_2 atmosphere under full spectrum light. To prepare the working electrodes, catalysts are dropped onto an indium tin oxide (ITO) glass. Briefly, 5 mg catalysts are suspended in 0.5mL ethanol solution with 1wt % nafion. Subsequently, the slurries are coated on the ITO glass uniformly, and heated at 333K in vacuum over 12h.

Apparent quantum efficiency (AQE) measurement

The apparent quantum efficiency (AQE) measured process is essentially as good as the photocatalytic N_2 fixation experiments except that under different monochromatic light wavelengths (365 nm, 420 nm, 520 nm and 625 nm) irradiation using the filters with a bandwidth of ± 5 nm and 50 mg photocatalyst in 100 ml deionized water. The values of light intensities are measured by a photo radiometer. The catalytic reactions for determining AQE are carried out in a quartz vessel with the irradiation area of 1 cm^2. The AQE is calculated as following equation:

$$AQE = \frac{Number\ of\ generated\ NH_3 * 3}{Number\ of\ incident\ photons} = \frac{n_{NH3} \times N_A \times 3}{\frac{W \times A \times t}{h \times v}}$$

Where n_{NH3} is the molar number of generated NH_3; N_A and h are the he Avogadro's constant and Planck constant; W, v, A and t are the irradiation light intensity, frequency, irradiation area and time, respectively.

Density functional theory calculations

The Materials Studio software is used for Density functional theory (DFT)

calculations. The Perdew-Burke-Erzenhof (PBE) function in generalized gradient approximation (GGA) is applied to determine the exchange correlation energy, and a vacuum thickness of 15 Å is adopted to separate it from its periodic model. The cutoff energy and k-point grid are site at 500 eV and 2 × 2 × 1 in structural optimization process. Furthermore, the convergence criterion of total energy and residual force are 1×10^{-5} eV and 0.03 eV/Å, respectively. Here, a TiO_2 model with the (101) surface system is applied. Three-Layer models are used with 2 lower layers fixed and 1 upper layer relaxed. For the doped system, it is constructed by replacing a Ti atom with Pt from the pure phase system, and the carbon dots are adsorption on the surface. All N_2 adsorption is selected to take place above the metallic active sites.

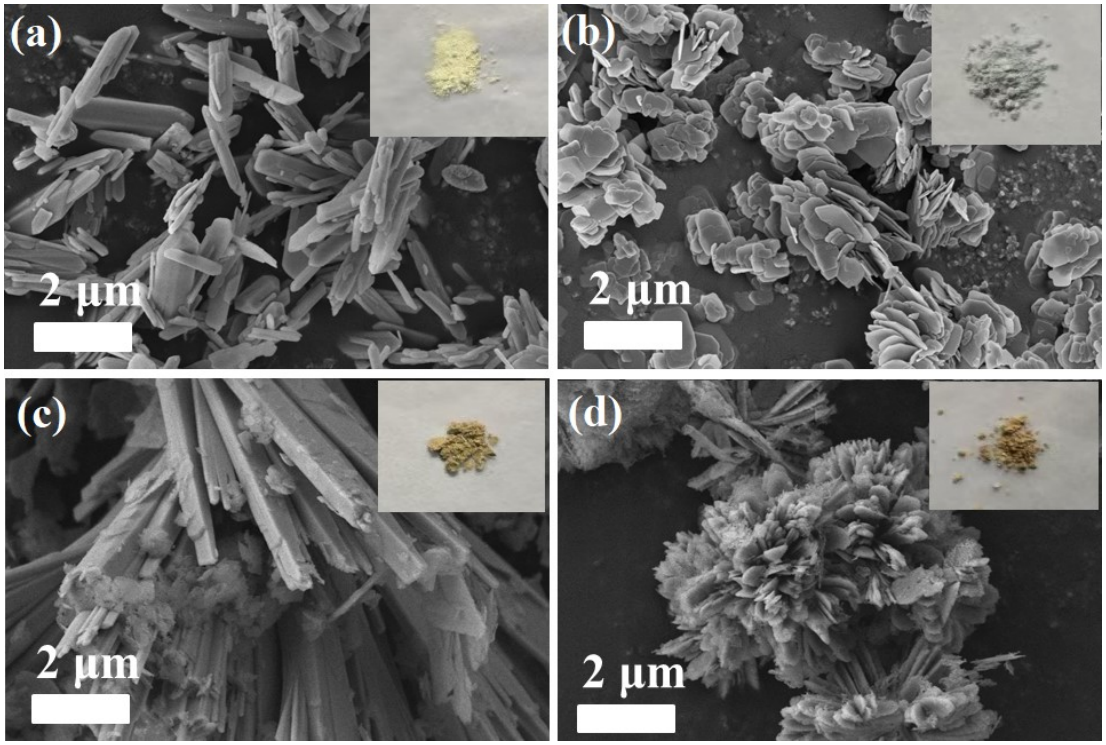

Fig.S1 Apparent and microstructures of the samples. (a) CO; (b) MO; (c) CM-3; (d) CCM-3

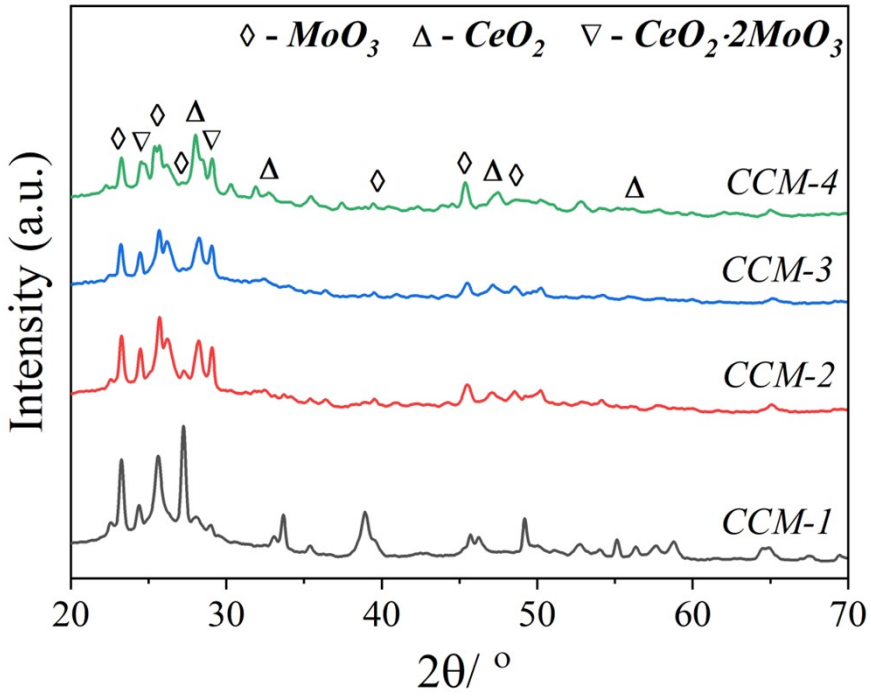

Fig.S2 XRD patterns of the various catalysts

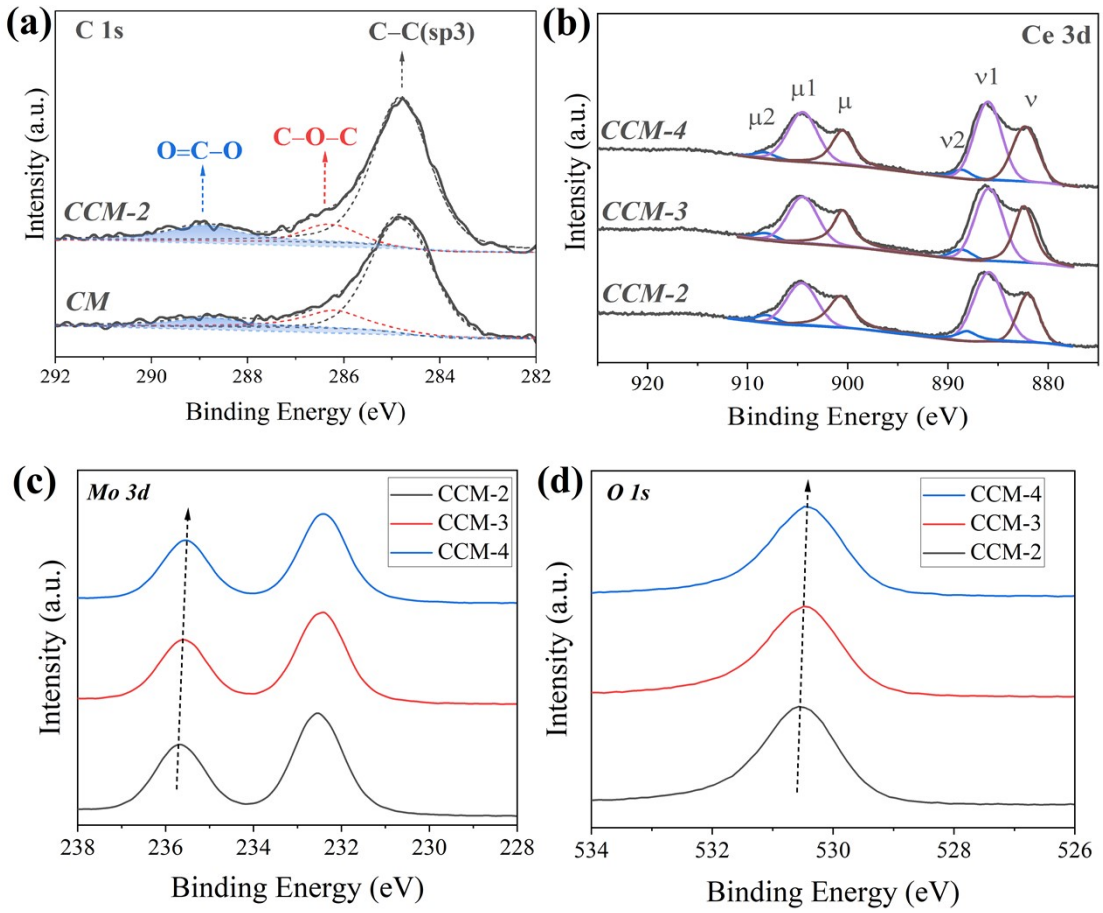

Fig.S3 XPS curves of C1s (a), Ce 3d (b), Mo 3d (c) and O 1s (d) for the various hetero-junction samples

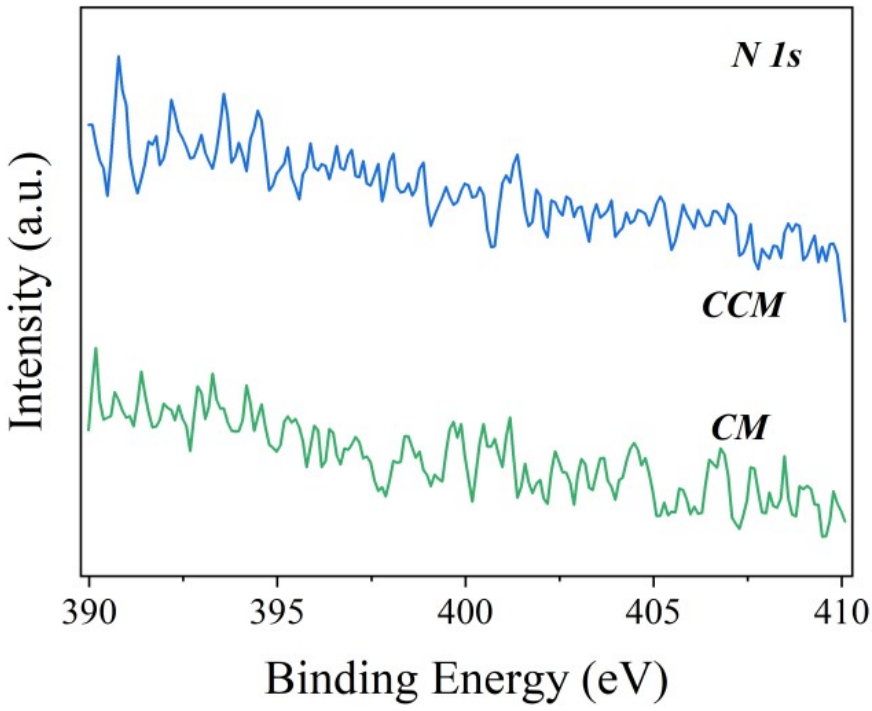

Fig.S4 N 1s XPS curves for the CM and CCM samples

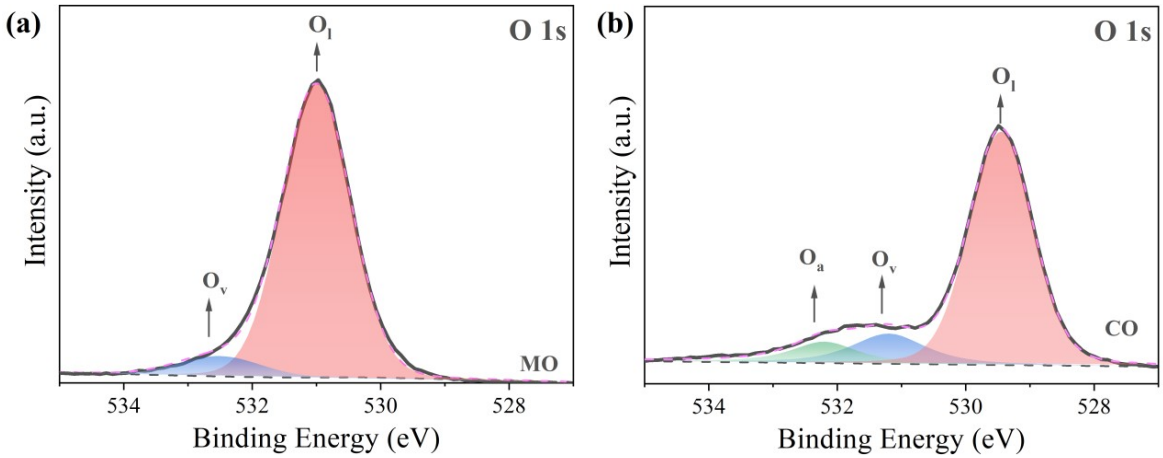

Fig.S5 O 1s XPS curves for the original (a) MoO_{3-x} and (b) CeO_2

The O_v fraction of 11.9% in CO sample and 7.4 % in MO are also lower than of 12.8% in the carbonization-derived heterojunction (CCM) based on the XPS peaks area.

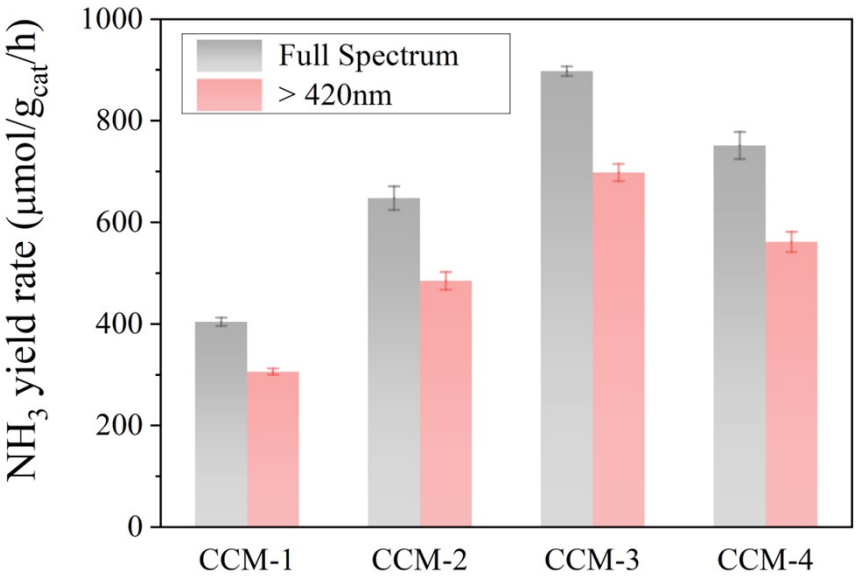

Fig.S6 NH_3 yield rates of the various photocatalysts

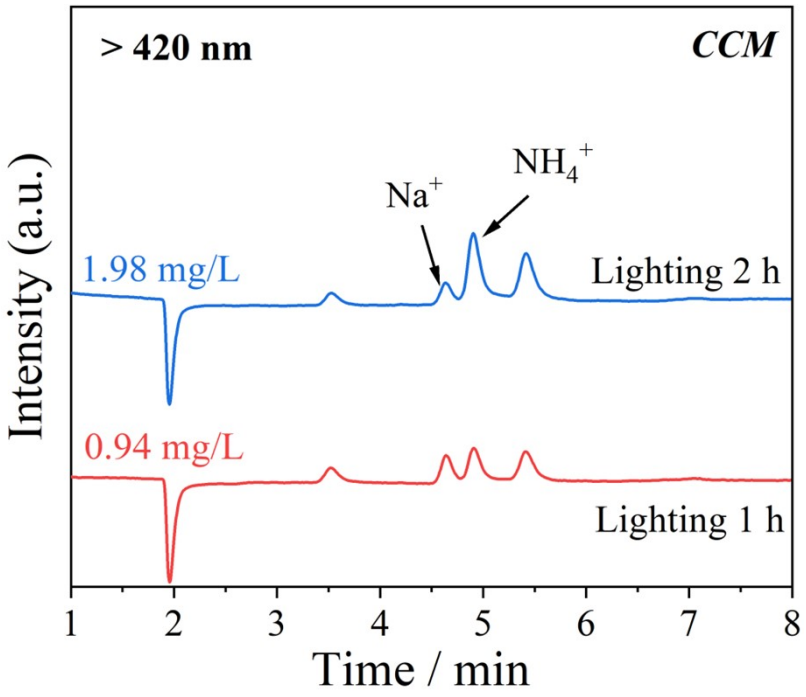

Fig.S7 Ion chromatography results of NH_4^+ from N_2 photo-fixation over the CCM sample under visible light for 20mg samples in 250ml deionized water.

To further confirm the ammonia formation, ion chromatograph (IC) measurement is also applied to detect the NH_4^+. The intensity of NH_4^+ peak increases with the lighting time. The calculated ammonia produced rate of 687 μmol/g/h basically corresponds to the result of 698 μmol/g/h obtained by the Nessler's reagent method.

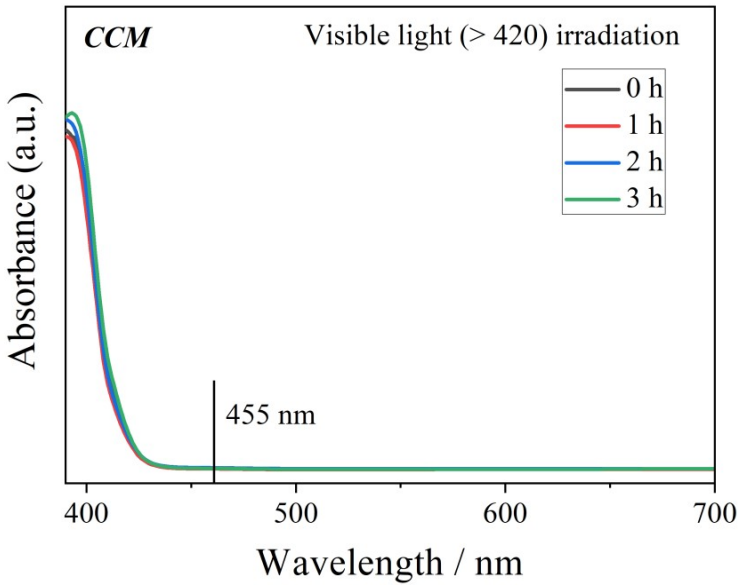

Fig.S8 UV-vis absorption curves of 180 min reaction solution after adding Watt-Chrisp reagent for the NH_2-NH_2 detection.

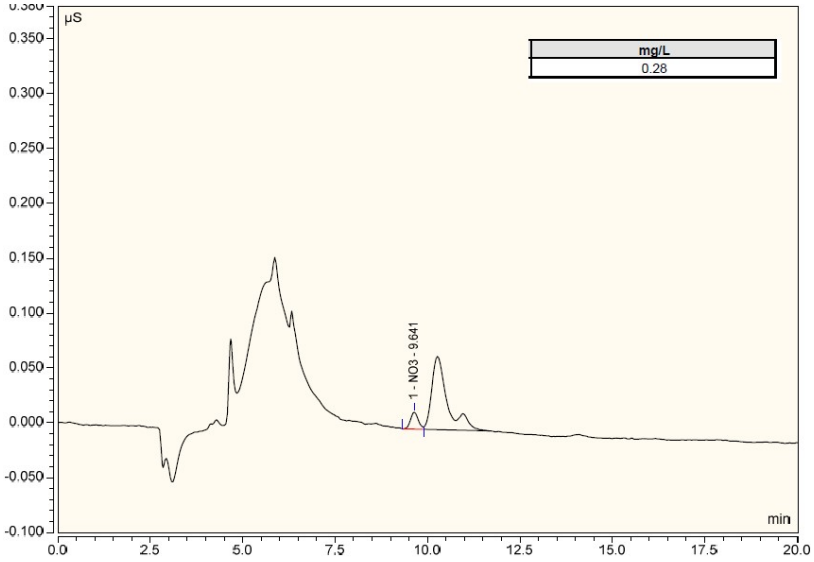

Fig.S9 Ion chromatography results of NO_3^+ from N_2 photo-fixation for the CCM sample under visible light with 20mg samples in 250ml deionized water over 2 h.

Hydrazine (N_2H_4) is the initial by-product during the photocatalytic N_2 fixation, and the N_2H_4 production is also detected through the Watt-Chrisp method. We cannot find any signal at 455 nm in the UV-vis absorption curves of 3 h photoreaction solution over the CCM sample in Fig.S7, indicating no by-product hydrazine during the photocatalytic process. Moreover, another by-product of NO_3^- ion in oxidation half-reaction was also concerned through ion chromatograph method in Fig.S8. IC

characterization shows that a small amount of NO_3^- with 0.28 mg/L is generated over the CCM sample under visible light irradiation for 2 h. Herein, a sustainable conversion of N_2 molecules into ammonia and nitrate products is achieved in this system.

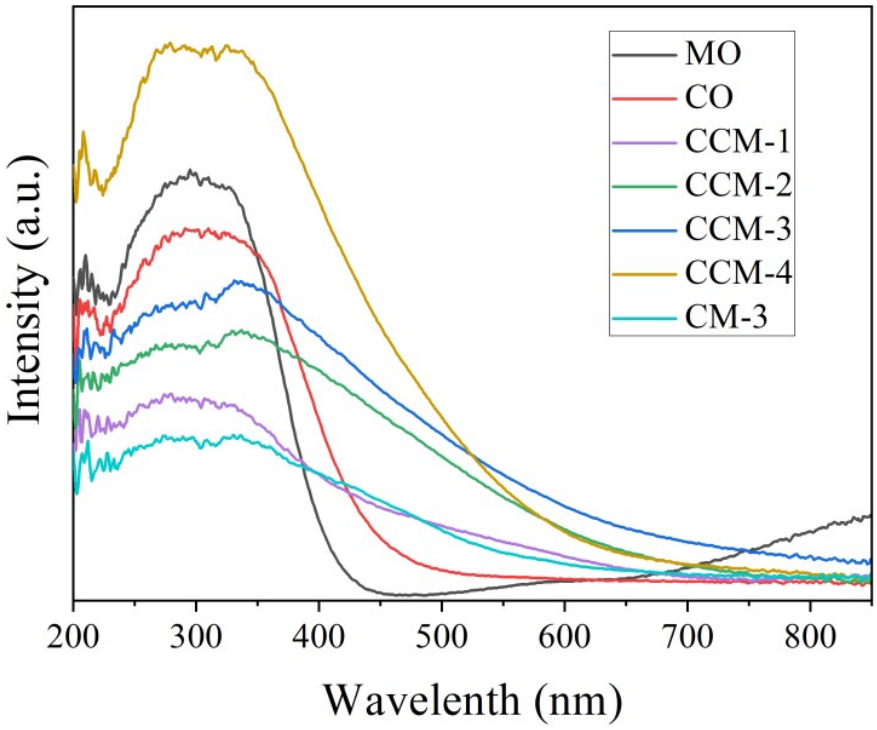

Fig.S10 UV-vis diffuse reflectance spectra for the various photocatalysts

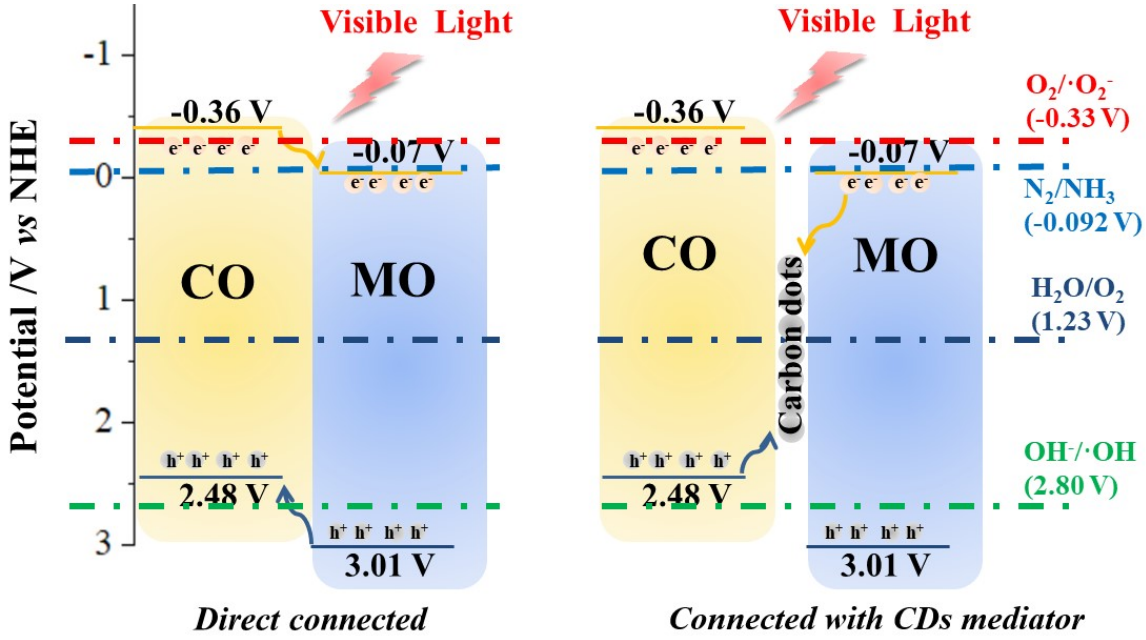

Fig.S11 The connection mode of the heterojunction structure

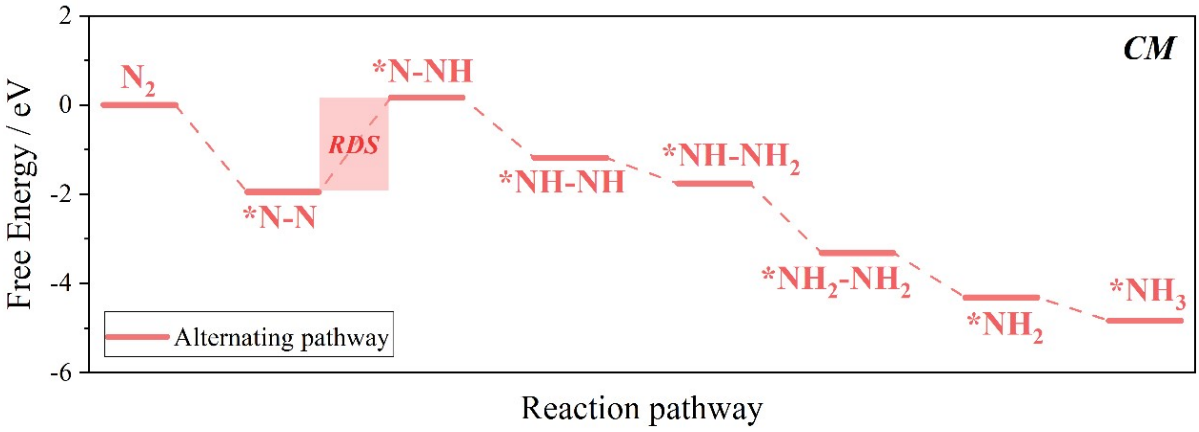

Fig.S12 the reaction pathway for the hydrogenation process of N_2 to NH_3 over the CM sample

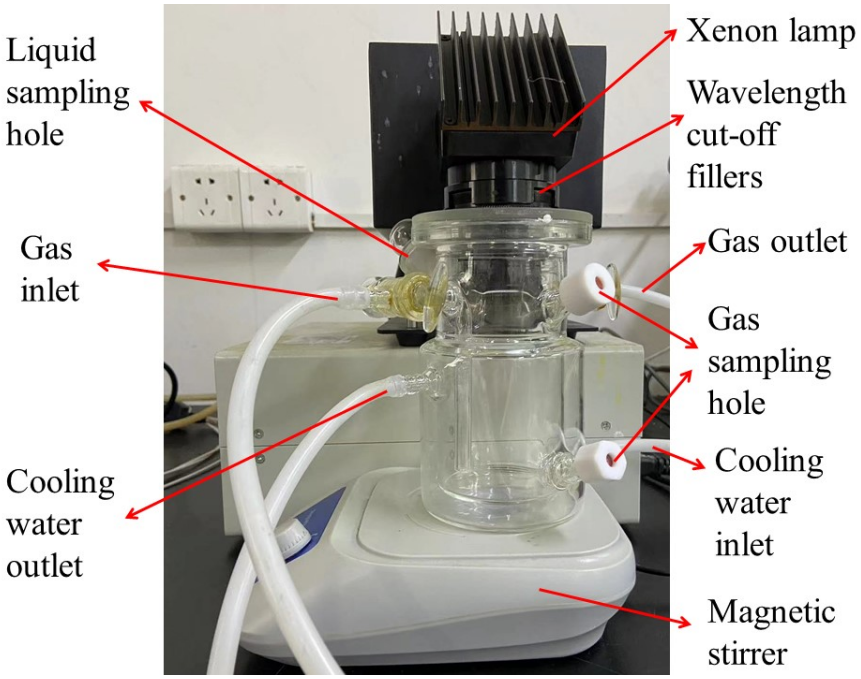

Fig.S13 Photoreactor

Table.S1 The calculated volume-averaged particle sizes by the Scherrer analysis

Catalysts and components	MoO_3 (nm)	CeO_2 (nm)
MO	19.8 ± 0.3	\
CO	\	13.5 ± 0.5
CCM-1	20.1 ± 0.7	\
CCM-2	22.7 ± 0.5	20.0 ± 0.4
CCM-3	30 ± 1.5	19.4 ± 0.5
CCM-4	25.2 ± 1.2	18.9 ± 0.5

Table.S2 The selected results of N_2 photofixation under 300 W Xe lamp irradiation in the recent reports for the similar catalysts

Catalysts	Sacrificial agent	Light source	NH_3 rate ($\mu mol \cdot g_{cat}^{-1} \cdot h^{-1}$)	Ref.
CCM-3	No	Full spectrum	897	This work
CCM-3	No	> 420 nm	698	This work
TiO_2/Bi/CC	No	Full spectrum	165	3
TiO_2-Au-BiOI	No	Full spectrum	54.4	4
FeN-CDs/TiO_2@CN	methanol	Full spectrum	550.9	5
Cu-EMMOH	No	Full spectrum	210	6
$Bi_2Sn_2O_7$/BiOBr	No	Full spectrum	459	7
$Co(OH)_2$/CeO_2/CDs	No	Full spectrum	232	8
TiO_2/$SrTiO_3$/g-C_3N_4	Methanol	Full spectrum	219	9
Bi_2S_3/OV-Bi_2MoO_6	No	> 420 nm	50.4	10
WS_{2-x}/La_1-$WO_{2.9}$	Methanol	Full spectrum	124.6	11
$BiFeO_3$-TiO_2-CNT	No	Full spectrum	150.8	12
MZ-600	No	Full spectrum	103.9	13

References

1. G. W. Watt and J. D. Chrisp, *Analytical Chemistry*, 1952, **24**, 2006-2008.
2. T. Dambrauskas and H. H. Cornish, *American Industrial Hygiene Association journal*, 1962, **23**, 151-156.
3. Y. Li, R. Li, Z. Sun, L. Guo, Y. Wang, X. Ma, H. Li, T. Lei, C. Fan and J. Liu, *Journal of colloid and interface science*, 2024, **664**, 198-209.
4. X. J. Yu, H. R. Qiu, Z. Wang, B. Wang, Q. N. Meng, S. D. Sun, Y. F. Tang and K. Zhao, *Applied Surface Science*, 2021, **556**.
5. K. Li, C. Sun, Z. Q. Chen, H. X. Qu, H. F. Xie and Q. Zhong, *Chemical Engineering Journal*, 2022, **429**.
6. H. Zhang, Y. Chen, Y. Pan, L. Bao and J.-y. Ge, *Journal of Colloid and*

Interface Science, 2023, **642**, 470-478.

7. Y. Zhang, J. Di, X. Zhu, M. Ji, C. Chen, Y. Liu, L. Li, T. Wei, H. Li and J. Xia, *Applied Catalysis B-Environment and Energy*, 2023, **323**, 122148.
8. H. W. Zhang, Y. F. Chen, L. Bao and J. Y. Ge, *Journal of Colloid and Interface Science*, 2023, **634**, 642-650.
9. R. Tao, X. H. Li, X. W. Li, C. L. Shao and Y. C. Liu, *Nanoscale*, 2020, **12**, 8320-8329.
10. Y. Zhang, L. Guo, Y. Wang, T. Wang, T. Ma, Z. Zhang, D. Wang, B. Xu and F. Fu, *Journal of Materials Science & Technology*, 2022, **110**, 152-160.
11. K. Y. Shi, C. L. Yu, J. Yuan, W. Y. Huang, K. Q. Lu, Z. C. Zhuang, J. R. Huo, Y. Xie, E. R. Zhang, D. S. Wang and K. Yang, *Applied Catalysis B-Environment and Energy*, 2025, **376**.
12. E. Fekri, M. S. S. Dorraji and M. Vahedpour, *Fuel Processing Technology*, 2025, **275**.
13. R. X. Hao, Z. H. Zheng, Y. X. Li, M. L. Zheng, S. Q. Pan, J. Hu and H. Huang, *Journal of Catalysis*, 2025, **447**.